Uniaxial-Stress Control of Spin-Driven Ferroelectricity in Multiferroic $Ba_2CoGe_2O_7$

Taro Nakajima,[1,*] Yusuke Tokunaga,[1] Vilmos Kocsis,[1,2] Yasujiro Taguchi,[1]
Yoshinori Tokura,[1,3] and Taka-hisa Arima[1,4]

[1]*RIKEN Center for Emergent Matter Science (CEMS), Wako 351-0198, Japan*
[2]*Department of Physics, Budapest University of Technology and Economics and Condensed Matter Research Group of the Hungarian Academy of Sciences, Budapest H-1111, Hungary*
[3]*Department of Applied Physics and Quantum-Phase Electronics Center (QPEC), University of Tokyo, Tokyo 113-8656, Japan*
[4]*Department of Advanced Materials Science, University of Tokyo, Kashiwa 277-8561, Japan*

(Received 29 September 2014; published 10 February 2015)

We have demonstrated that spin-driven ferroelectricity in a tetragonal multiferroic $Ba_2CoGe_2O_7$ is controlled by applying uniaxial stress. We found that the application of compressive stress along the [110] direction leads to a 45° or 135° rotation of the sublattice magnetization of the staggered antiferromagnetic order in this system. This allows the spontaneous electric polarization to appear along the c axis. The present study suggests that an application of anisotropic stress, which is the simplest way to control symmetry of matter, can induce a variety of cross-correlated phenomena in spin-driven multiferroics.

DOI: 10.1103/PhysRevLett.114.067201 PACS numbers: 75.85.+t, 77.80.-e, 77.84.-s

Ferroelectricity induced by magnetic ordering has been one of the major topics in condensed matter physics since the pioneering work on $TbMnO_3$ [1], which exhibits cycloidal magnetic orderings accompanied by the ferroelectricity [2,3]. The key to the emergence of the spin-driven ferroelectricity is symmetry breaking due to the magnetic ordering [2,4]. Even when neither the crystal nor magnetic structure has a polar nature, a combination of their symmetry possibly induces the ferroelectricity [5]. Because the symmetry of the magnetic structures can be easily controlled by applying a magnetic field, there have been a lot of reports on magnetic-field-control of spin-driven ferroelectricity in multiferroics [1,6–10]. It is also demonstrated that an application of an electric field can be used to control magnetic orders [11,12], in particular spin helicity, i.e., clockwise or counterclockwise (left-handed or right-handed) arrangement of the spins, in the multiferroics with helimagnetic orderings [13–17]. However, there remains another and the most primitive way to control the symmetry of the system, that is, application of anisotropic stress. In the present study, we have demonstrated that spin-driven ferroelectricity in multiferroic $Ba_2CoGe_2O_7$ can be controlled by application of uniaxial stress.

$Ba_2CoGe_2O_7$ has a tetragonal crystal structure belonging to the space group of $P\bar{4}2_1m$, which represents a noncentrosymmetric but nonpolar structure [18]. As shown in Fig. 1(a), the magnetic Co^{2+} ions form a square lattice in the ab plane. Below the magnetic phase transition temperature of $T_N = 6.7$ K, this system exhibits an antiferromagnetic ordering with the magnetic propagation wave vector of $\boldsymbol{Q} = (1, 0, 0)$ [19,20]. The magnetic moments on the Co sites lie in the ab plane in the antiferromagnetic phase because of an easy-plane type single-ion anisotropy. In addition, a recent neutron scattering study by Soda *et al.* has shown the existence of small in-plane anisotropy which aligns the magnetic moments parallel to the a or b axis [21]. Note that the a and b axes are equivalent to each other for

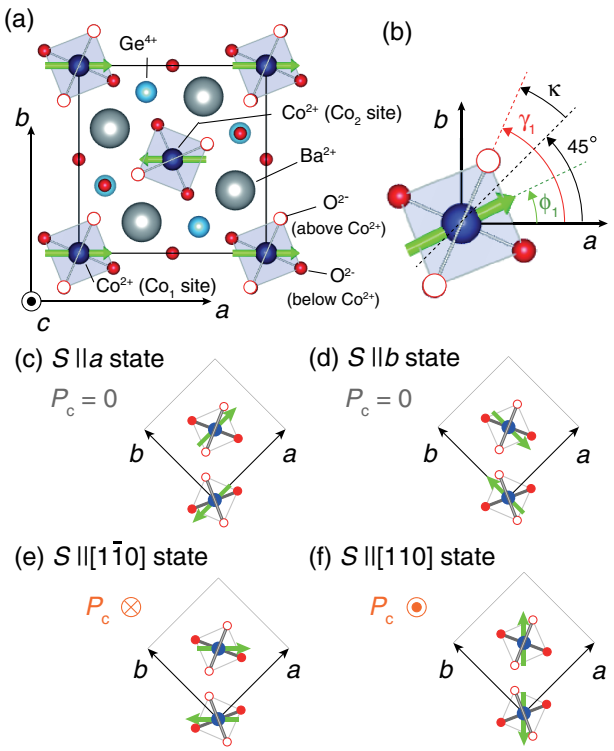

FIG. 1 (color online). (a) Crystal structure of $Ba_2CoGe_2O_7$ with the magnetic structure in the ground state. (b) Definitions of ϕ_i and γ_i for $i = 1$. (c)–(f) Schematics of the spin arrangements of (c) $S\|a$, (d) $S\|b$, (e) $S\|[1\bar{1}0]$ and (f) $S\|[110]$ states.

the tetragonal crystal as shown in Fig. 1(a). In Figs. 1(c) and 1(d), we show magnetic structures in the ground state. In this Letter, we refer to these magnetic states as the $S\|a$ state and $S\|b$ state, respectively. These states also have weak ferromagnetic moments perpendicular to the c axis owing to the Dzyaloshinskii-Moriya (DM) interaction arising from the lack of inversion symmetry.

This compound is also known as a spin-driven multiferroic [22,23]. While the ground state does not have the ferroelectricity, an application of a magnetic field induces electric polarization. Murakawa *et al.* [23] have revealed that the magnetic-field variations of the electric polarization are well described by the spin-dependent p-d hybridization mechanism [5], in which a local electric dipole moment for a Co–O bond, $\boldsymbol{p}$, is given by $\boldsymbol{p} \propto (\boldsymbol{S}\cdot\boldsymbol{e})^2\boldsymbol{e}$, where $\boldsymbol{S}$ and $\boldsymbol{e}$ are the spin moment on the Co site and the unit vector for the Co–O bonding direction, respectively. By assuming that the spins lie on the ab plane, the net electric polarization along the c axis, P_c, is given by

$$P_c \propto \sum_{i=1,2} \cos 2(\phi_i - \gamma_i), \tag{1}$$

where the indices $i = 1$ and 2 stand for the two Co sites (Co_1 and Co_2) in a unit cell, and ϕ_i denotes an angle between the spin moment on the Co_i site and the a axis. The definition of an angle γ_i for the case of $i = 1$ is shown in Fig. 1(b). Note that the CoO_4 tetrahedra are alternatingly rotated around the c axis by $\pm\kappa(= 24°)$ from the [110] direction, and therefore γ_1 and γ_2 are given by $\pi/4 + \kappa$ and $\pi/4 - \kappa$, respectively. Applying Eq. (1) to the $S\|a$ and $S\|b$ states, one can find that the Co_1 and Co_2 sites have electric dipole moments with the same magnitudes but opposite signs [21]. When an external magnetic field of ~0.4 T is applied along the [110] direction below T_N, the spins are rotated to be perpendicular to the [110] direction, as shown in Fig. 1(e). This leads to the electric polarization along the c axis. We refer to the field-induced ferroelectric state as the $S\|[1\bar{1}0]$ state. Similarly, an application of magnetic field along the $[1\bar{1}0]$ direction induces the $S\|[110]$ state shown in Fig. 1(f), in which the polarity of P_c is opposite to that in the $S\|[1\bar{1}0]$ state [23].

These previous results have shown that the spin-driven ferroelectricity in this system is closely related to the directions of the spins. Because the estimated in-plane anisotropy is as small as ~0.2 μeV [21], the spin-dependent electric polarization can be controlled not only by applying a magnetic field, but also by applying uniaxial stress, which may affect the magnetic anisotropy through deformations of the crystal. We thus performed electric polarization measurements on this system under applied uniaxial stress and magnetic fields.

A single crystal of $Ba_2CoGe_2O_7$ was grown by the floating-zone method and cut into a rectangular shape with dimensions of $2.9 \times 2.6 \times 1.1$ mm^3. The widest surfaces were normal to the c axis, and silver-paste electrodes were formed on these surfaces to observe P_c. We employed a top-loading type vertical-uniaxial-stress insert [24,25]. As illustrated in the inset of Fig. 2(a), the sample was placed between ZrO_2 pistons in the stress cell attached on the bottom of the insert. We also employed a horizontal-uniaxial-stress cell illustrated in the inset of Fig. 3(b). In both setups, the uniaxial compressive stress ($\sigma_{[110]}$) was applied along the [110] direction [26]. The uniaxial-stress

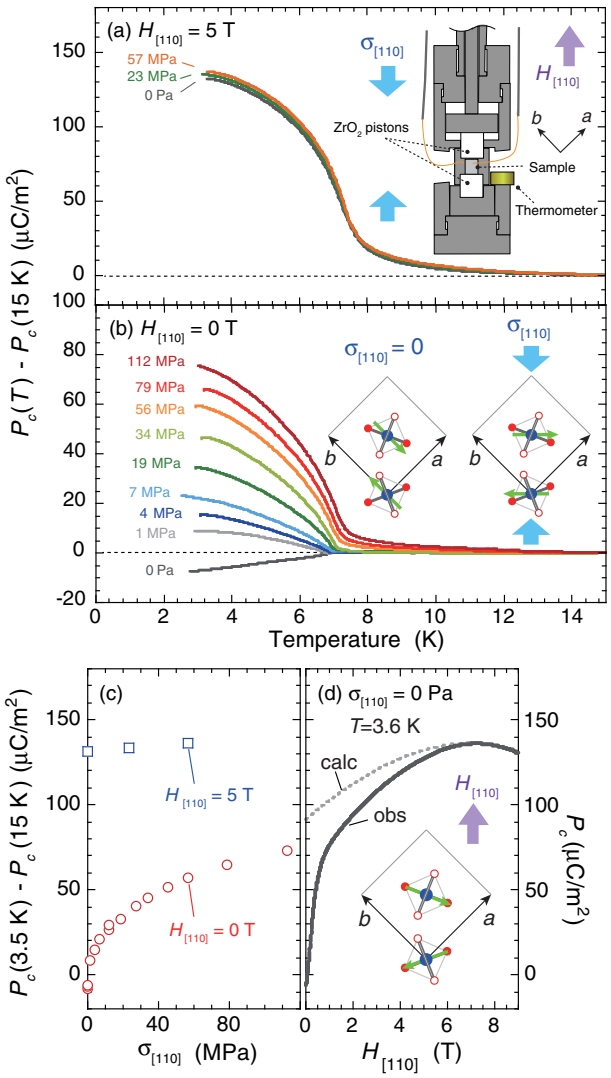

FIG. 2 (color online). [(a),(b)] Temperature variations of P_c measured on cooling with various compressive stress $\sigma_{[110]}$ (a) under $H_{[110]} = 5$ T and (b) 0 T. The insets of (a) and (b) are an illustration of the vertical-uniaxial-stress cell and schematics showing the $\sigma_{[110]}$-induced change of the magnetic structure, respectively. (c) The $\sigma_{[110]}$ dependences of the values of P_c at $T = 3.5$ K under $H_{[110]} = 0$ and 5 T. (d) The $H_{[110]}$-variations of P_c measured under $\sigma_{[110]} = 0$ (solid line) and calculated by substituting the $H_{[110]}$ dependence of the magnetization into Eq. (1) [23].(dotted line). The inset shows the magnetic structure under $H_{[110]}$ of about 6 T.

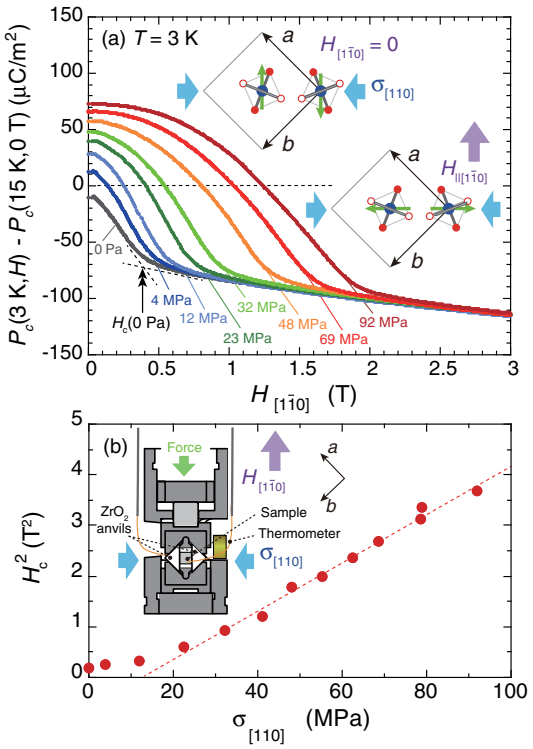

FIG. 3 (color online). (a) $H_{[1\bar{1}0]}$-variations of P_c measured with increasing $H_{[1\bar{1}0]}$ under various compressive stress $\sigma_{[110]}$. The initial values of P_c were determined by the pyroelectric measurements in zero magnetic field. The double black arrow indicate the 'knee point' for the P_c-$H_{[1\bar{1}0]}$ curve for $\sigma_{[110]} = 0$. The insets schematically show the change in magnetic structure under applied $\sigma_{[110]}$ and $H_{[1\bar{1}0]}$. (b) The $\sigma_{[110]}$ dependence of a square of H_c at $T = 3$ K. A dotted line is a guide for the eyes. The inset shows an illustration of the horizontal uniaxial-stress cell.

insert was loaded into a Physical Property Measurement System (Quantum Design, Inc.). External magnetic fields of up to 9 T were applied along the vertical direction, which corresponds to the [110] and $[1\bar{1}0]$ directions in the measurements with the vertical- and horizontal-uniaxial-stress cells, respectively. We measured displacement electric current with varying temperature (T), magnetic fields applied along the [110] and $[1\bar{1}0]$ directions ($H_{[110]}$ and $H_{[1\bar{1}0]}$) and $\sigma_{[110]}$, using an electrometer (Keithley 6517B). By integrating the current with respect to time, we deduced P_c.

We performed pyroelectric measurements with the vertical-uniaxial-stress cell in zero magnetic field and under applied magnetic field of $H_{[110]} = 5$ T. Before each measurement, the uniaxial stress was applied at 15 K. In Fig. 2(a), we show the temperature variations of P_c under $H_{[110]} = 5$ T. Similarly to the previous studies [22,23], P_c was observed to emerge below T_N, which is slightly shifted toward higher values under the applied magnetic field. The magnitude of P_c at $\sigma_{[110]} = 0$ is consistent with that in the previous studies [22,23]. We found that the application of $\sigma_{[110]}$ hardly affects the temperature variation of P_c under $H_{[110]} = 5$ T. In zero magnetic field, by contrast, P_c remarkably increases with increasing $\sigma_{[110]}$, as shown in Fig. 2(b). We also found that the polarity of the $\sigma_{[110]}$-induced P_c in zero magnetic field is the same as that of the $H_{[110]}$-induced P_c. This suggests that the application of $\sigma_{[110]}$ stabilizes the $S\|[1\bar{1}0]$ state in zero magnetic field [27], as shown in the inset of Fig. 2(b).

Figure 2(c) shows the values of P_c at $T = 3.5$ K under $H_{[110]} = 0$ and 5 T as functions of $\sigma_{[110]}$. In zero magnetic field, P_c saturates at around 80–90 μC/m^2 in the high uniaxial-stress limit, and it does not seem to reach the value measured under $H_{[110]} = 5$ T (~130 μC/m^2). This can be understood in terms of the p-d hybridization model as follows. According to Eq. (1), the magnitude of P_c is maximized when the condition of $\phi_i = \gamma_i$ (or $\phi_i = \gamma_i + \pi/2$) is satisfied for both of $i = 1$ and 2. Murakawa *et al.* have pointed out that this situation is realized when the system has uniform magnetization along the [110] direction [23], because the CoO_4 tetrahedra are tilted by $\pm\kappa$, as shown in the inset of Fig. 2(d). In fact, P_c is maximized around 6 T, as seen in the $H_{[110]}$ variation of P_c measured under $\sigma_{[110]} = 0$ [Fig. 2(d)]. By using the value of P_c at 6 T and Eq. (1), we can estimate P_c of the zero-field $S\|[1\bar{1}0]$ state, in which the spins on the Co_1 and Co_2 sites are nearly parallel (or antiparallel) to the $[1\bar{1}0]$ direction, to be 90 μC/m^2 [28]. This is in good agreement with the saturation value of P_c in zero magnetic field.

Figure 3(a) shows the $H_{[1\bar{1}0]}$ dependence of P_c measured with the horizontal-uniaxial-stress cell at 3 K. We found that the sign of P_c is reversed by application of $H_{[1\bar{1}0]}$, except for the data measured with $\sigma_{[110]} = 0$. This indicates that the $\sigma_{[110]}$-induced $S\|[1\bar{1}0]$ state turns into the $S\|[110]$ state under applied $H_{[1\bar{1}0]}$, as illustrated in the insets of Fig. 3(a). Here, we defined a 'knee point' in a P_c-$H_{[1\bar{1}0]}$ curve as the critical magnetic field (H_c) for the transition from the zero-field states to the $S\|[110]$ state, as shown in Fig. 3(a). We found that H_c monotonically increases with increasing $\sigma_{[110]}$, and there is a linear relationship between H_c^2 and $\sigma_{[110]}$ above ~10 MPa, as shown in Fig. 3(b). On the other hand, the Zeeman energy at H_c is also proportional to H_c^2; specifically, it is estimated to be $-\frac{1}{2}\chi_{[110]}H_c^2$, where $\chi_{[110]}$ is the magnetic susceptibility for the $S\|[110]$ state, by assuming that the magnetization curve is linear in the field induced $S\|[110]$ state above H_c. Therefore, the observed $\sigma_{[110]}$ dependence of H_c^2 implies that the energy difference between the $S\|[1\bar{1}0]$ state and the $S\|[110]$ state is proportional to $\sigma_{[110]}$.

It should be noted that this system has piezoelectricity even above T_N. This is because the application of $\sigma_{[110]}$ breaks the fourfold rotoinversion and twofold screw symmetry of the crystal structure, allowing the piezoelectric

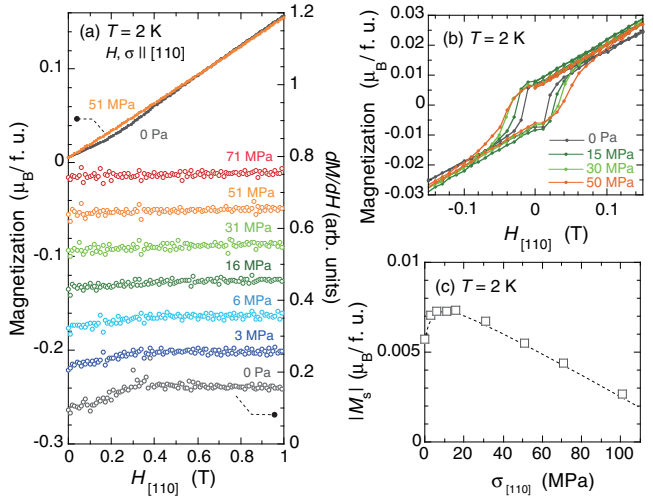

FIG. 4 (color online). (a) Magnetization curves and dM/dH, (b) hysteresis loops of the magnetization, and (c) spontaneous magnetization measured at 2 K under various $\sigma_{[110]}$. Note that the dM/dH data are vertically shifted by 0.1 for each, in order to enhance the visibility. The dotted line in (c) is a guide for the eyes.

polarization to appear along the c axis. Therefore, the observed values of P_c shown in Figs. 2(a)–2(c) and 3(a) are not absolute values, but the relative changes from $T = 15$ K. By measuring the piezoelectric responses at various temperatures and magnetic fields, we have confirmed that the piezoelectric polarization from the crystal is independent of temperature and applied magnetic field (see the Supplemental Material [29]). This ensures that the relative changes of P_c correspond to the T, $H_{[1\bar{1}0]}$, and $\sigma_{[110]}$ variations of the spin-dependent electric polarization.

To directly observe the effect of uniaxial stress on the magnetic order, we measured magnetization under applied uniaxial stress using the Magnetic Property Measurement System (Quantum Design, Inc.). We employed another uniaxial-stress insert developed for the magnetization measurements [25]. The directions of the applied uniaxial stress and magnetic fields were parallel to the [110] direction. Figure 4(a) shows the M-H curves and their derivatives measured with various $\sigma_{[110]}$ at 2 K. In zero uniaxial stress, the dM/dH shows a kink around 0.4 T. This anomaly corresponds to the transition from the $S\|a$ or $S\|b$ state to the $S\|[1\bar{1}0]$ state [21]. We found that the kink in dM/dH is gradually smeared out with increasing $\sigma_{[110]}$, and almost disappears above $\sigma_{[110]} \sim 16$ MPa. These results are in accord with our interpretation that the application of $\sigma_{[110]}$ stabilizes the $S\|[1\bar{1}0]$ state in zero magnetic field.

Here, we discuss the effect of the uniaxial stress from the microscopic point of view. In the previous inelastic neutron scattering study, Soda *et al.* have proposed the spin Hamiltonian for this system, which consists of the exchange interactions, the DM interaction, the Zeeman term, the easy-plane type single-ion anisotropy, and the weak in-plane anisotropy called "spin-nematic interaction" [21]. The present results suggest that the application of $\sigma_{[110]}$ introduces an additional in-plane anisotropy term whose magnitude is proportional to $\sigma_{[110]}$; specifically, $E\sigma_{[110]}\sum_i[(S_i^{[110]})^2 - (S_i^{[1\bar{1}0]})^2]$, where E is the proportional constant, and $S_i^{[110]}$ and $S_i^{[1\bar{1}0]}$ are the spin components along the [110] and $[1\bar{1}0]$ directions, respectively. Combining the $\sigma_{[110]}$ dependence of H_c^2 shown in Fig. 3(b) and the magnetization curves shown in Fig. 4(a), we can estimate ES^2 to be ~ 0.1 μeV/MPa. This means that the application of $\sigma_{[110]} \sim 2$ MPa should induce the $[1\bar{1}0]$-direction anisotropy comparable to the spin-nematic interaction estimated to be ~ 0.2 μeV [21]. This is consistent with the high sensitivity of P_c to $\sigma_{[110]}$ in zero magnetic field.

The effect of the $\sigma_{[110]}$-induced anisotropy can be also seen in hysteresis loops of the magnetization measured at 2 K. Figure 4(b) shows that the coercive force is enhanced by the application of $\sigma_{[110]}$. In addition, the spontaneous magnetization ($|M_s|$) due to the weak ferromagnetism decreases with increasing $\sigma_{[110]}$, as shown in Fig. 4(c). These results qualitatively agree with the increasing in-plane anisotropy.

In conclusion, we have demonstrated that the magnetic order and ferroelectricity in the multiferroic $Ba_2CoGe_2O_7$ can be controlled by applying uniaxial stress. We have revealed that the application of uniaxial stress along the [110] direction affects the magnetic anisotropy of the Co^{2+} ions. As a result, the directions of the spin moments are rotated from the a and b axes to the $[1\bar{1}0]$ direction, and consequently the spin-driven electric polarization emerges along the c axis in zero magnetic field. While this uniaxial-stress control of the magnetic order as well as the spin-driven electric polarization also may be applicable to a variety of spin-driven multiferroics such as the representative compound $TbMnO_3$, we suggest that this technique will be most effective when the crystal structure has relatively high symmetry and the application of the uniaxial stress results in distinct changes in the symmetry. For example, a similar square-lattice multiferroic compound CuB_2O_4 [11,30] potentially exhibits pronounced uniaxtial stress responses with respect to the spin, lattice, and dielectric degrees of freedom.

The authors thank A. Kikkawa and C. Terakura for useful discussions on the development of the uniaxial-stress cells. We also thank S. Bordács and I. Kézsmárki for fruitful discussions. This work was supported by Grants-in-Aid for Young Scientists (A) (No. 25707032) and (B) (No. 25800203), the Funding Program for World-Leading Innovative R&D on Science and Technology (FIRST Program) on Quantum Science on Strong Correlation from JSPS, Japan, and Hungarian Research Funds OTKA K108918.

*taro.nakajima@riken.jp

[1] T. Kimura, T. Goto, H. Shintani, K. Ishizaka, T. Arima, and Y. Tokura, Nature (London) **426**, 55 (2003).

[2] M. Kenzelmann, A. B. Harris, S. Jonas, C. Broholm, J. Schefer, S. B. Kim, C. L. Zhang, S.-W. Cheong, O. P. Vajk, and J. W. Lynn, Phys. Rev. Lett. **95**, 087206 (2005).

[3] Y. Yamasaki, H. Sagayama, N. Abe, T. Arima, K. Sasai, M. Matsuura, K. Hirota, D. Okuyama, Y. Noda, and Y. Tokura, Phys. Rev. Lett. **101**, 097204 (2008).

[4] M. Mostovoy, Phys. Rev. Lett. **96**, 067601 (2006).

[5] T. Arima, J. Phys. Soc. Jpn. **76**, 073702 (2007).

[6] N. Hur, S. Park, P. A. Sharma, J. S. Ahn, S. Guha, and S.-W. Cheong, Nature (London) **429**, 392 (2004).

[7] T. Kimura, G. Lawes, T. Goto, Y. Tokura, and A. P. Ramirez, Phys. Rev. B **71**, 224425 (2005).

[8] Y. Yamasaki, S. Miyasaka, Y. Kaneko, J.-P. He, T. Arima, and Y. Tokura, Phys. Rev. Lett. **96**, 207204 (2006).

[9] G. Lawes *et al.*, Phys. Rev. Lett. **95**, 087205 (2005).

[10] K. Taniguchi, N. Abe, T. Takenobu, Y. Iwasa, and T. Arima, Phys. Rev. Lett. **97**, 097203 (2006).

[11] M. Saito, K. Ishikawa, S. Konno, K. Taniguchi, and T. Arima, Nat. Mater. **8**, 634 (2009).

[12] Y. Tokunaga, Y. Taguchi, T.-h. Arima, and Y. Tokura, Nat. Phys. **8**, 838 (2012).

[13] Y. Yamasaki, H. Sagayama, T. Goto, M. Matsuura, K. Hirota, T. Arima, and Y. Tokura, Phys. Rev. Lett. **98**, 147204 (2007).

[14] S. Seki, Y. Yamasaki, M. Soda, M. Matsuura, K. Hirota, and Y. Tokura, Phys. Rev. Lett. **100**, 127201 (2008).

[15] I. Cabrera *et al.*, Phys. Rev. Lett. **103**, 087201 (2009).

[16] M. Soda, K. Kimura, T. Kimura, M. Matsuura, and K. Hirota, J. Phys. Soc. Jpn. **78**, 124703 (2009).

[17] T. Nakajima, S. Mitsuda, S. Kanetsuki, K. Tanaka, K. Fujii, N. Terada, M. Soda, M. Matsuura, and K. Hirota, Phys. Rev. B **77**, 052401 (2008).

[18] V. Hutanu, A. Sazonov, H. Murakawa, Y. Tokura, B. Náfrádi, and D. Chernyshov, Phys. Rev. B **84**, 212101 (2011).

[19] A. Zheludev, T. Sato, T. Masuda, K. Uchinokura, G. Shirane, and B. Roessli, Phys. Rev. B **68**, 024428 (2003).

[20] T. Sato, T. Masuda, and K. Uchinokura, Physica B **329–333**, 880 (2003).

[21] M. Soda, M. Matsumoto, M. Månsson, S. Ohira-Kawamura, K. Nakajima, R. Shiina, and T. Masuda, Phys. Rev. Lett. **112**, 127205 (2014).

[22] H. T. Yi, Y. J. Choi, S. Lee, and S.-W. Cheong, Appl. Phys. Lett. **92**, 212904 (2008).

[23] H. Murakawa, Y. Onose, S. Miyahara, N. Furukawa, and Y. Tokura, Phys. Rev. Lett. **105**, 137202 (2010).

[24] T. Nakajima, S. Mitsuda, T. Nakamura, H. Ishii, T. Haku, Y. Honma, M. Kosaka, N. Aso, and Y. Uwatoko, Phys. Rev. B **83**, 220101 (2011).

[25] T. Nakajima *et al.*, J. Phys. Soc. Jpn. **81**, 094710 (2012).

[26] The loads applied on the uniaxial-stress cells were monitored by a load meter, similarly to the previous works [24,25]. The magnitudes of $\sigma_{[110]}$ applied using the vertical-uniaxial-stress cell were directly deduced from the loads. As for the horizontal-uniaxial-stress cell, we calibrated the magnitudes of $\sigma_{[110]}$ by measuring P_c in zero magnetic field.

[27] In zero magnetic field, the finite negative P_c was observed at $\sigma_{[110]} = 0$. This might be ascribed to a small residual stress in the sample or stress from the glue used to fix the sample on the piston.

[28] Although in the zero-field $S \| [1\bar{1}0]$ state, there are two magnetic domains with weak ferromagnetic moments parallel and antiparallel to the [110] direction, respectively, both of them induce the electric polarization in the same direction. Therefore, the magnitude of the $\sigma_{[110]}$-induced P_c does not depend on the magnetic domain structure.

[29] See Supplemental Material at http://link.aps.org/supplemental/10.1103/PhysRevLett.114.067201 for the results of the piezoelectric measurements.

[30] N. D. Khanh, N. Abe, K. Kubo, M. Akaki, M. Tokunaga, T. Sasaki, and T. Arima, Phys. Rev. B **87**, 184416 (2013).